Third International Conference on Geotextiles, 1986, Vienna, Austria

BACOT, J., COULET, Ch. et GIELLY, J., Institut Universitaire de Technologie I, Lyon, France

EVALUATION OF THE ANCHORING CAPACITY OF A SUPPLE REINFORCEMENT BY MEANS OF AN EXPONENTIAL LAW

ERMITTLUNG DER VERANKERUNGSKRÄFTE EINER PLASTISCHEN EINLAGE MITTELS EINER EXPONENTIALGLEICHUNG

EVALUATION DE LA CAPACITE D'ANCRAGE D'UNE INCLUSION SOUPLE PAR UNE LOI DE FROTTEMENT EXPONENTIELLE

A soil massif acquires new mechanical properties when geotextiles or geomembranes are inserted into it. It might be valuable to take into account the increase in the mechanical properties of the "soil-reinforcement". The very high suppleness of the reinforcement which are used means that those inclusions are corrugated. It will then be incorrect to consider the soil inclusion interface as a geometrically perfect plane and impossible to estimate the strength in the plane of the inclusion with a linear friction law. We show that the exact shape of the interface can largely explain why the value of the soil reinforcement friction coefficient when it is measured using shearing laboratory tests (Casagrande box giving f_o), or in situ tests (pull-out tests giving f^*), are so different.
We give an analytical expression of f_o^* function of f_o, and of parameters characteristic of the interface shape (corrugation effect); experimental results obtained in laboratory and in situ are given.

INTRODUCTION

A soil massif acquires new mechanical properties when geotextiles are inserted into it. In addition to the modification of the soil massif hydrolic regime, the presence of geotextiles - taken in the sense of being reinforcements as well - can generate new mechanical properties, generally of higher values. Therefore, it can be interest to take into account this improvement of the soil-inclusion set, thus increasing the profitability of any operation making use of geotextiles.

Such a preoccupation is of course important for the project-conceptors.

Here we only investigate the "mechanical properties improvement" of the soil massif.

It should be remarked, first of all, that the presence of geotextiles improves the mechanical performance of the soil, this being due to the primary effect of the geotextile : control of the hydrolic discharges resulting in a dispersal of the interstitial pressures harmful to the soil bearing-capacity. But as these geotextile drains have their own mechanical resistance, their insertion into the soil can be seen as a "direct reinforcement" as well.

The mechanical properties of geotextiles is well known, numerous tests having been made in laboratories as well in situ.

We believe that the testing conditions at failure are generally quite different from the reality. When the tests are being done in laboratories, the geotextiles are being put in position very carefully : the interfaces are almost plane and the compacting is homogeneous.

The soil-geotextile interaction is measured, for example, in terms of friction : a "soil-geotextile friction coefficient" will be defined. Most of the testing conditions derive from the Casagrande box test (modified to some extent); at times the test changes into that of a pull-out test of the geotextile in relation to the soil massif. In that case, the strip is laid in a well defined plane, this being done to simplify the calculation of the soil-geotextile friction coefficient (linear friction, uniform vertical stress, etc...).

In a soil massif set down in layers, the soil-geotextile interface is never perfectly plane, neither is it perfectly horizontal (Fig. 1). However small these defects are, they do not in the least create problems as concerns the anchoring of the geotextile in the soil massif.

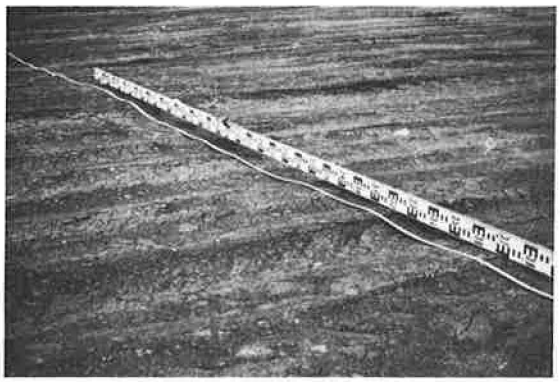

Figure 1 : Visualization of the corrugation

Knowing the geotextiles suppleness, it is easily conceived that they will hug exactly the defects in planeness existing in soil-layers. When it is covered by the overlying layer, the geotextile will keep the initial profile. It will have become corrugated.

If the gectextile is not very supple (reinforced geotextiles of the FILTRAM 16 or 131 types) the corrugation phenomenon can still take place provided that the vertical load - made up of the geotextile's own weight and the result of compacting - presses down the reinforced geotextile onto the underlying-layer.

We expose here the theory of supple reinforcement corrugation and the principle of the tension calculation at any point of the geotextile, in addition to the results of the tests carried out in laboratoty on a bidimensional model (unidirectional corrugation) and in situ. These last ones are conditioned by the measuments of the surface irregularities caused by the tamping compactors (Fig. 2).

Figure 2: Corrugation resulting from compacting

PRINCIPLE OF THE THEORY

The main idea is to consider that the corrugated reinforcement behaves towards the soil surrounding it like a rope around a bollard. The winding of the rope around the bollard participates in the strain that is applied to the rope (in the limit of the rope's capacity) in the proportion "a hen to an egg". We will then consider the reinforcement as a succession of windings, the curvatures being sometimes upward, sometimes downward (alternate windings), and take into account the total deviation θ_T of the whole of the corrugations, AB being a representation of the geotextile's track along a vertical section of the massif (Fig. 3).

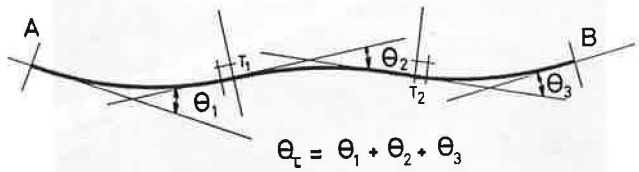

Figure 3 : Evaluation of the total deviation from A to B

LAW OF EXPONENTIAL FRICTION

Let us consider a cylindrical bearing surface and a ribbon (e.g. a geotextile) able to slide on a surface. A force T_1 is exerted on one of the ribbon's extremities. A force T_2 must be in action at the other extremity; we are going to calculate this force so that the ribbon will start sliding on the cylinder. The friction coefficient of the ribbon is on the cylindrical bearing surface is $f_o = tg\ _o$. The ribbon is in contact along a length AB and θ is the winding angle.

The equilibrium of a small curvilinear element GG' of the ribbon is governed by the following equations :

$$ds = r.d\alpha \qquad F_t = F_n.f_o \qquad dT/T = f_o.d\alpha$$

from which we get : $\ln(T_2/T_1) = f_o.\theta$

and then : $T_2 = T_1.\ \exp\ (f_o.\theta)$

This explains how important loads can be sustained when many turns are taken around the cylinder while strains of very small or even nil value are exerted at the other end of the ribbon.

This property can be adapted to our case, with the following equivalences :

to the ribbon correspond the geotextile
to the cylinder the soil surface
to the winding angle corresponds the total deviation θ_T along the geotextile.

APPLICATION TO THE CASE OF A GEOTEXTILE
(bidimensional problem)

Let us consider a fictitious ribbon belonging to a thin inclusion (very long geotextile whose width is the unit). We have a curving element of this ribbon and its length AB = ds (Fig. 4).

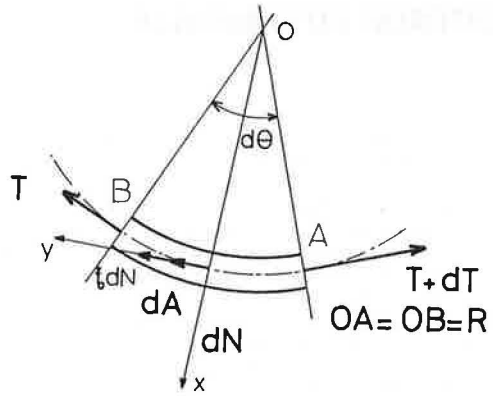

Figure 4 : Equilibrium of a ribbon section.

This geotextile is in position inside a soil massif whose internal friction angle is φ_{SI} (this value can be measured with the modified shearing box). We will suppose that the inclusions corrugates in a series of circular arcs (Fig. 4).

τ_a is the adhesion stress between the soil and the inclusion. The element AB is subject to a difference of tension between the points B and A. In a bidimensional environment, the increase in tension is due :

- to the soil-inclusion adhesion $dA = p.\tau_a.ds$ (the ribbon perimeter p = twice the width)
- to the friction resulting from the reaction of the soil on the inclusion.

$$f_o.dN \qquad \text{with} \qquad f_o = tg\,\varphi_{SI}$$

The equilibrium of the element AB comes out, in projection on Ox as :

$$T.\ \sin(d\theta/2) + (T + dT).\sin(d\theta/2) - dN = 0$$

If $d\theta$ is very small, we get : $T = dN/d\theta$ (1)

In projection on Oy :

$$T.\ \cos(d\theta/2) - (T + dT).\cos(d\theta/2) + f_o.N + dA = 0$$

but $ds = r.d\theta$

When we integrate over an angular arc at the centre θ, we obtain :

$$T_B = T_A.\frac{1}{\exp(f_o.\theta)} - \frac{p.R.\tau_a}{f_o}\left(1 - \frac{1}{\exp(f_o.\theta)}\right) \qquad (2)$$

This equation expresses the fact that it is possible to determine the length AB - or θ - and we otherwise know the force between A and B.

When it is used in layer form, the inclusion (geotextile or geomembrane) has a function of reinforcement. In the vertical section of the figure 5 we try to determine the force T in relation to a free extremity (T = 0).

The curvature radii are marked from 1 to 3 in decreasing strains, and the successive deviation angles from θ_1 to θ_3 If the anchoring strain brings T to an equilibrium, the strain at the free extremity of the inclusion will be nil.

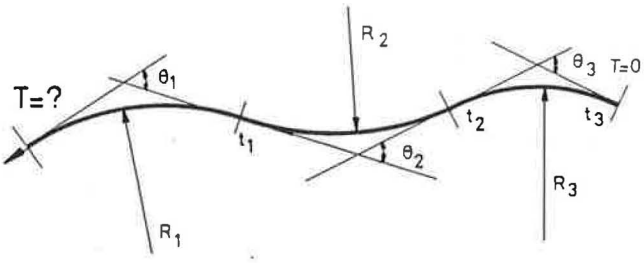

Figure 5 : Calculation of the available strain T function of the inclusion distortion characteristics.

We set down :

$$\alpha_i = \frac{1}{\exp(f_o.\theta_i)} \quad \text{and} \quad \alpha_i' = 1 - \alpha_i$$

By successively applying the equation (2) between the inflexion points t_1, t_2, ... and by generalising, we have :

$$T = p.\tau_a.\sum_1^n \frac{\alpha_i.R_i}{\alpha_1.\alpha_2\cdots\alpha_n} \qquad (3)$$

To simplify, let us now suppose that the corrugation is regular : $R_1 = R_2 = \ldots = R$.

The equation (3) becomes :

$$T = p.\tau_a.R.\frac{\alpha'}{\alpha}(\theta_i)\sum_0^{n-1}\frac{1}{\alpha_i} \qquad (4)$$

(n = number of successive deviations)

The force due to adhesion can be considered as the force necessary to sta rt the sliding movement.

σ_v being the average vertical stress acting on the inclusion, if we look at it from the point of view of an elementary surface $\tau_a = f_o . \sigma_v$

The equation (3) can then be written (with p = 2 twice the width of the ribbon) :

$$T = 2.1.R.\ \sigma_v.((\exp(\theta_i.f_o) - 1)\sum_1^n \exp\left[(\theta_i.f_o)(i-1)\right] \qquad (5)$$

(for a ribbon length equal to the unit)

If the ribbon does not corrugate (law of linear friction)

$$T = 2.1.\ \sigma_v.f_o \qquad (6)$$

In this case the fictitious ribbon having a length equal to the unit (length AB) and the deviation between A and B being nil, by analogy between (5) and (6), we obtain :

$$\exp\ (f_o.\theta_o - 1) = f_o$$

or :

$$\theta_o = \frac{1}{f_o}\ln\ (1 + f_o) \qquad (7)$$

θ_o is called "contact deviation" and allows the pure friction f_o to be interpreted in terms of angular deviation transmitted along the ribbon.

The calculation of T with the help of (6) can be done with an apparent length of the ribbon L* equal to the real length L. The apparent length is measured along a straight line passing through both extremities of the inclusion. Thus the corrugated ribbon shows an apparent length very close to the real or developped length. With an arc subtending a chord of 0.50 m and a rise of 1 cm, (Fig. 6), we have :

$\widehat{ACB}$ = 50.05 cm ; AB = 50 cm ; CH = 1 cm

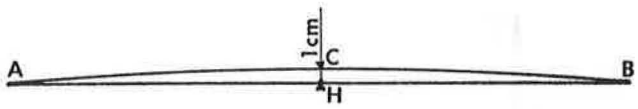

Figure 6: Arc-chord-rise relation

The angle at the center is 9°16 and the radius is 313m. Hence the approximation is excellent. In the most unfavoble cases (CH = 3cm), the error stays below 2%.

PRACTICAL DETERMINATION OF THE COEFFICIENT f_o TO BE TAKEN INTO ACCOUNT FOR THE CALCULATION OF THE MAXIMUM ANCHORING STRAIN.

From (6) and (7) we get:

$$T = 2.\sigma_v.1.L.\exp((\theta_o + \theta_T)f_o - 1) \qquad (8)$$

The equation (8) allows the direct calculation of the value of T for a traction test on an inclusion in position in the soil , it is at any rate possible to estimate the value of θ_T, which is the"apparent geometrical deviation".

If L, the real length of the inclusion, is taken into account, we get:

$$T = 2.\sigma_v.1.L.f_o$$

EXPERIMENTAL DETERMINATION OF θ_T

θ_T is the total angular deviation ($\theta_T = \Sigma\theta_i$) for an inclusion of length L. In the following we will fix the unit of angular deviation θ_L as that of an inclusion whose leng length is the unit (generaly the meter).

Thus:

$$\theta_T = L.\theta_L$$

The evaluation of θ_L as done as follow:

Making use of the opportunity of existing excavation works, we plotted a few hundred meters of transverse profile after a tamping compactor DYNAPAC CP 22 (7 tyres, 7 tonnes unladen weight) had gone over the ground. The spacing between wheels was 28 cm, the distance between the axels was 50 cm, the width of the special smooth tyres was 28 cm and the tyres pressure was chosen to be 5.10^5 Pa.

We used a level and a surveyor's rod which was moved along a chain placed at the perpendicular from the track of the earth roller to plot the exact profile. If we assume that an inclusion as supple as the ribbon can hug exactly the profile that had been plotted and if we calculate the mean measurement of all the values of θ_L that were determined from the ground plotting, we estimate the value of θ_L to be 0.216 rd/m (Diagram 1).

As an illustrative calculation we will take (unfavorable hypothesis) θ_L = 0.2 rd/m with L = 10m.

In the case of an inclusion having a pure friction coefficient f_o with the soil of 0.4, an apparent friction coefficient f_o is deduced:

1/ with the help of the equation (8):

$$\theta_T = L.\theta_L = 0.2\ \text{rd/m} \times 10\text{m} = 2\text{rd}$$

$$\theta_o = 1/f_o\ \ln(1+f_o) = 1/0{,}4\ \ln(1+0{,}4) = 0{,}841$$

and $f_o^* = 0{,}745$

2/ with the help of the graph of the figure 7. For an abscissa θ_T = 2rd, we read f_o^* = 0,75 on the curve f_o = 0,4

Thus an apparent friction coefficient of 0.745 is given when the corrugating is taken into account, almost twice as much in the present case, and this has been checked

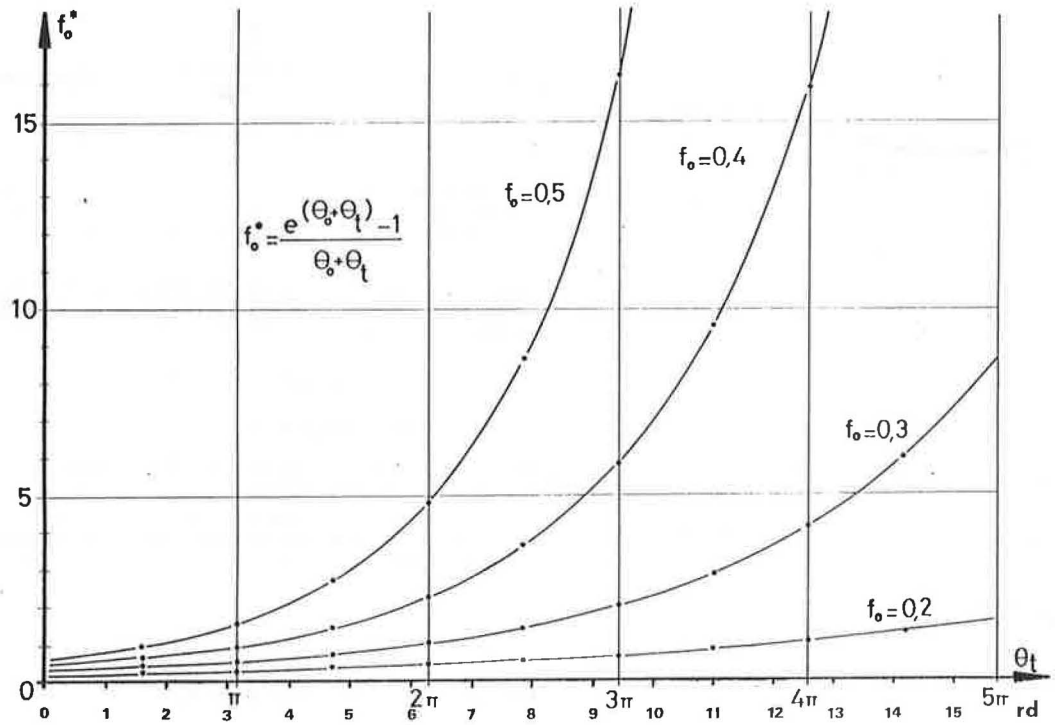

Figure 7: Graph showing the value of f_o function of the total angular deviation θ_T.

during pull-out tests on reinforced soil reinforcement, as well as on a bidimensional scaled-down model, for which the theoretical and experimental results are given below.

CHECKING OF THE THEORY ON A BIDIMENSIONAL SCALED-DOWN MODEL.

At the same time as a search for experimental results dealing with the behaviour of real inclusions put into position in earth-works, wheter definitively or not, we have undertaken to check the validity of the corrugation theory with the help of a bidimensional scaled-down model having the following characteristics:

- the soil is represented by polished mild-steel rollers of ∅ = 20 mm, and length L = 59 mm.
- the inclusion is represented by steel foil (thickness varying from 0.05 mm to 0.3 mm) with a working surface separating the initial environment into two distinct zones without any contact between them (Fig. 8) The rollers are placed along a hexagonal mesh and steel ribbon is going to corrugate.

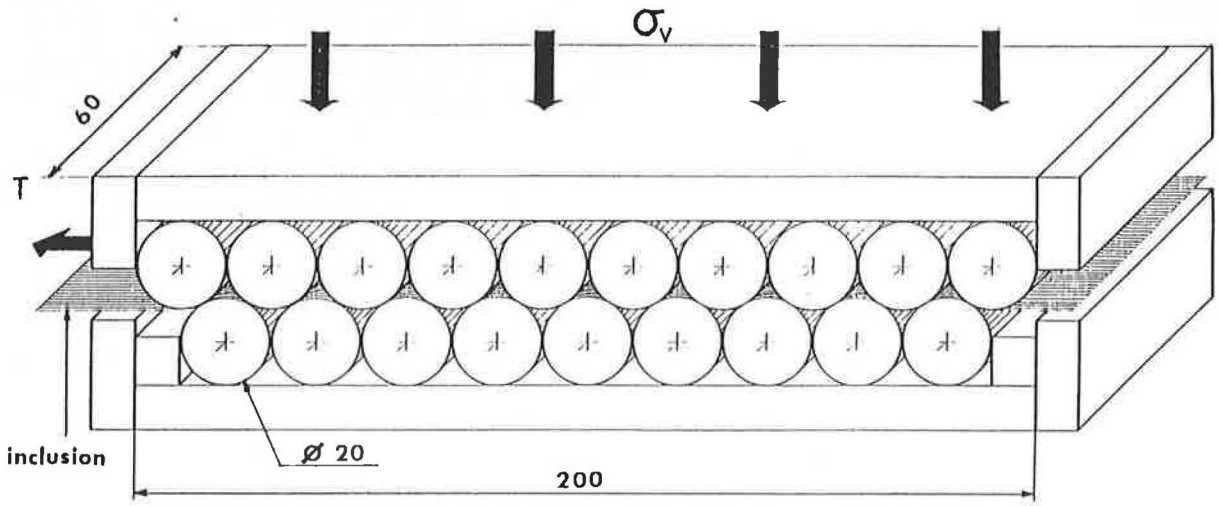

Figure 8 : Bidimensional scaled-down model designed to study the pull-out strain on a corrugated inclusion

The whole is placed inside a specially designed box that can be fixed on a rectlinear shearing machine of the M O type. The tests were conducted so as to extract an inclusion from the environment (the rollers) and were beforehand vertically charged. The vertical movements are free under the influence of the traction force T exerted at the head of the inclusion. The amplitude of the initial corrugation receiving the vertical strain was measured for every inclusion (Fig. 9).

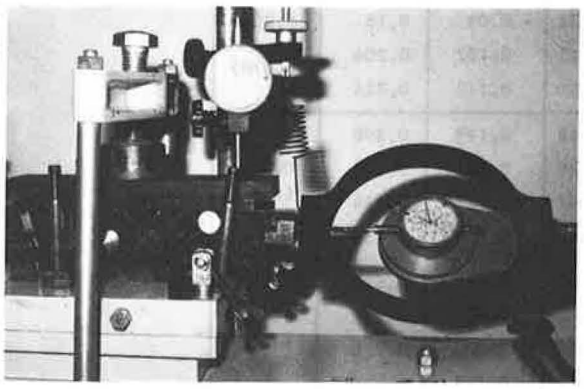

Figure 9 : Bidimensional scaled-down model fixed on an M&O shearing box.

The analysis of the results consists in comparing the experimental values Texp for each of the inclusions to the theorical values T calculated in this application, according to the equation (8), with $f_o = 0.2$.
($f_o = 0.2$: mild-steel/foil pure friction)

The results are shown in figure 10.

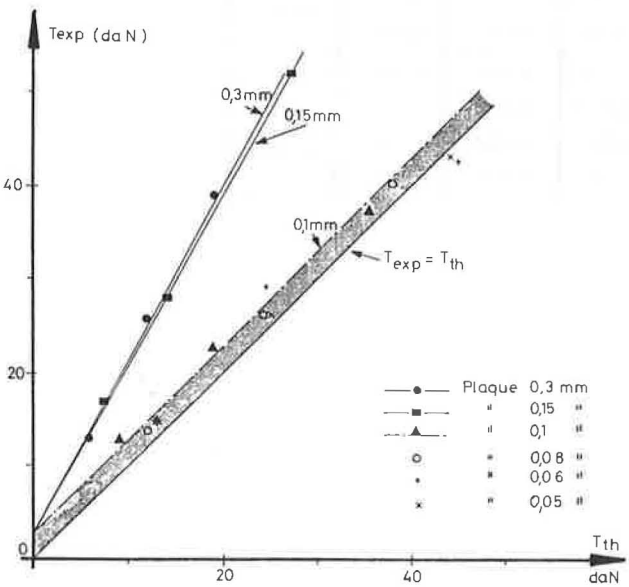

Figure 10 : Comparison between theoritical and experimental values.

The conditions of similarity and the respect of the condition $\theta_L = 0.2$ rd/m show that the only suitable inclusions are those with a thickness inferior or equal to 0.1 mm if we want to take into account the experimental results obtained on the bidimensional scale-down model, in view of the theory that we have just developped. The curves of the figure 10 clearly underline this restriction. The inclusions must possess an initial suppleness, so that the tension induced by corrugation can be considered as negligible, otherwise the reaction of the inclusion on the environment will induce an overstrain with a vertical resultant showing the increase of T_{exp} due to the friction.

Hence it is not true corrugation anymore but the superimposition of two effects: corrugation and dilatancy (which we have not mentioned).

CONCLUSION

The theoretical and experimental study of the "corrugation of supple inclusions" phenomenon leads to a fairly complete explaination of the differences observed between the values of the coefficients f_o and f measured respectively on the modified rectilinear shearing box and by pull-out tests. The influence of the shape of the soil inclusion interface is thus clearly brought to the for and the adoption of an elementary-friction law of an exponential type is proposed. A "theoretical apparent friction" parameter f_o^* is defined and will then be taken into account in a calculation of anchoring capacity instead of the coefficient f_o. This parameter can be superimposed on the dilatancy effect. When the theoretical and experimental values of the traction strain that can be summoned up in an inclusion are compared, the result is positive and allows us to conclude with the affirmative as to the existence of a "corrugation phenomenon", qualitatively as well as quantatively.

BIBLIOGRAPHICAL REFERENCE

(1) Bacot, J., "Contribution à l'étude du frottement entre une inclusion souple et un matériau pulvérulent Cas de la terre armée", Thèse de doctorat d'état, LYON, 30 septembre 1981.

Chart n° 1 : Summary of the values of θ_L (measured in situ), of the mean values and of the standard deviations.

		L (m)	θ_L °	θ_L rd	θ' (L) rd/m	θ (L) rd/m	Moyenne (s = écart type)
PROFIL 1	Avant compactage	3	17,18	0,3	0,1	0,2	0,202 (s = 0,018)
		6	30,87	0,532	0,09	0,18	
		9	52,45	0,915	0,102	0,204	
		12	77,15	1,346	0,112	0,224	
	Après 1er passage	3	25,65	0,448	0,149	0,298	0,246 (s = 0,037)
		6	41,68	0,728	0,121	0,242	
		9	55,43	0,967	0,107	0,214	
		12	79,23	1,383	0,115	0,230	
	Après 2e passage	3	23,13	0,404	0,135	0,270	0,235 (s = 0,026)
		6	36,88	0,644	0,107	0,214	
		9	56,11	0,98	0,109	0,218	
		12	81,29	1,419	0,118	0,236	
PROFIL 2	Après 2e passage	3	104,6	1,826	0,609	1,218	0,894 (s = 0,275)
		6	174,82	3,05	0,509	1,018	
		9	187,14	3,266	0,363	0,726	
		12	210,84	3,68	0,307	0,614	
PROFIL 3	Après 1er passage	3	14,66	0,256	0,085	0,17	0,181 (s = 0,019)
		6	28,18	0,492	0,082	0,164	
		9	46,50	0,812	0,09	0,18	
		12	71,47	1,247	1,04	0,208	
	Après 2e passage	3	23,12	0,403	0,134	0,238	0,216 (s = 0,016)
		6	36,87	0,643	0,107	0,214	
		9	51,07	0,891	0,099	0,198	
		12	73,75	1,287	0,107	0,214	